Title: Chronic CRH depletion from GABAergic, long-range projection neurons in the extended amygdala reduces dopamine release and increases anxiety

Authors: Nina Dedic[1,§], Claudia Kühne[1,§], Mira Jakovcevski[1], Jakob Hartmann[1,2], Andreas Genewsky[1], Karina S Gomes[1,3], Elmira Anderzhanova[1], Max L Pöhlmann[1], Simon Chang[1], Adam Kolarz[1], Annette M Vogl[1], Julien Dine[1], Michael W Metzger[1], Bianca Schmid[1], Rafael C Almada[1], Kerry J Ressler[2], Carsten T Wotjak[1], Valery Grinevich[4], Alon Chen[1], Mathias V Schmidt[1], Wolfgang Wurst[5,6,7], Damian Refojo[1,8], Jan M Deussing[1*]

Affiliations:

[1]Department of Stress Neurobiology and Neurogenetics, Max Planck Institute of Psychiatry, Munich, Germany

[2]Department of Psychiatry, Harvard Medical School and McLean Hospital, Belmont, MA, USA

[3]Laboratory of Neuropsychopharmacology – Paulista State University, Araraquara, Brazil

[4]Schaller Research Group on Neuropeptides, German Cancer Research Center, Central Institute of Mental Health, University of Heidelberg, Heidelberg, Germany

[5]Institute of Developmental Genetics, Helmholtz Zentrum München, [6]TU München, [7]DZNE, Munich, Germany

[8]Instituto de Investigacion en Biomedicina de Buenos Aires (IBioBA)-CONICET-Partner Institute of the Max Planck Society, Buenos Aires, Argentina

[§]These authors contributed equally to this work

***Correspondence author:**

Jan M. Deussing
Molecular Neurogenetics
Department of Stress Neurobiology and Neurogenetics
Max Planck Institute of Psychiatry,
Kraepelinstr. 2-10,
80804 Munich, Germany
Tel: +49 (0) 89-30622-639
Email: deussing@psych.mpg.de

Abstract: The interplay between corticotropin-releasing hormone (CRH) and the dopaminergic system has predominantly been studied in addiction and reward, while CRH-dopamine interactions in anxiety are scarcely understood. We describe a novel population of CRH-expressing, GABAergic, long-range-projecting neurons in the extended amygdala which innervate the ventral tegmental area, and alter anxiety following chronic CRH depletion. These neurons are part of a distinct CRH circuit which acts anxiolytic by positively modulating dopamine release.

Main Text:

CRH and its type 1 high affinity receptor (CRHR1) are widely distributed throughout the brain[1–3], and modulate neuroendocrine and higher order behavioral responses to stress[3]. Although it is widely accepted that CRH/CRHR1 signaling induces aversive stress-like behavioral responses, we and others have recently shown that CRH/CRHR1 can also act in an anxiolytic and appetitive manner via interaction with the dopaminergic system[1,4]. The ventral tegmental area (VTA) and substantia nigra pars compacta (SNc) express high levels of CRHR1[1,3], and conditional deletion of *Crhr1* in dopaminergic neurons increases anxiety and reduces dopamine release in the prefrontal cortex (PFC)[1], suggesting the presence of an "anxiolytic" CRH/CRHR1 circuit. However, the source of CRH in the VTA remains controversial[5–8]. Here we aimed to determine the origin and identity of VTA-targeting CRH neurons, and unravel their specific role in modulating positive emotional responses.

CRH is heavily expressed in structures of the extended amygdala including the anterior bed nucleus of the stria terminalis (aBNST) and the lateral part of the central amygdala (CeA)[2,3,9,10] two brain regions critically involved in the regulation of fear and anxiety[6,9–12]. In order to determine whether these CRH neurons project to the VTA, we injected AAVs expressing a Cre-dependent synaptophysin-GFP (Syp-GFP) fusion protein into different brain regions of of *Crh-ires-Cre* mice. Presynaptic Syp-GFP puncta in the VTA and SNc were most dense following tracer injection into the aBNST and CeA, (**Fig. 1a,b**; **Supplementary Fig. 1 and 2; Supplementary Table 1**), demonstrating the presence of VTA-innervating CRH neurons in the extended amygdala, which has also been suggested by others[13,14].

Double in situ hybridizations revealed an overwhelming majority of GABAergic CRH neurons in the aBNST/CeA, and confirmed[9,10] the distinct identity of *Gad65/67*-positive but largely *Pkcδ/Som*-negative CeA CRH neurons (**Fig. 1c, Supplementary Fig. 3 and 4a-c**). Contrastingly, most *Crh* neurons in the piriform cortex (Pir) co-expressed the glutamatergic marker *Vglut1*, while 29.9 ± 2.1% within the PVN co-localized with *Vglut2*, highlighting the

69 diversity of CRH neurons in different brain regions. Overall, these results suggest that VTA-
70 targeting CRH neurons of the aBNST/CeA represent GABAergic long-range projection
71 neurons.
72 Intriguingly, morphological assessment in *Crh-ires-Cre;Ai32(ChR2)* mice revealed the
73 presence of thin and mushroom-like dendritic spines in a subgroup of CRH neurons in the
74 aBNST and CeA (**Fig. 1d**). Dendritic spines are conventionally believed to be largely absent
75 from inhibitory neurons. Notably, we primarily detected aspiny GABAergic CRH neurons in
76 the hippocampus and cortex (**Supplementary Fig. 4d-f**), which have previously been
77 ascribed to classical, locally projecting interneurons including basket, chandelier, and double
78 bouquet cells[15,16].
79 Interestingly, we found that approximately one third of *Crh* neurons in the aBNST and CeA
80 co-express the calcium/calmodulin-dependent protein kinase 2 alpha (*Camk2a*) (**Fig 2a;**
81 **Supplementary Fig. 3**), one of the most abundant postsynaptic density proteins, which is
82 crucial for several aspects of synaptic plasticity[17], and predominantly expressed in excitatory
83 pyramidal neurons of the forebrain. Accordingly, *Crh*-expressing glutamatergic neurons in the
84 Pir also co-expressed *Camk2a* (**Supplementary Fig. 3**). However, CAMK2A signaling also
85 plays an important role in medium spiny neurons of the striatum[17,18], the most prominent
86 population of spiny, GABAergic, long-range projecting neurons in the brain. In addition,
87 VTA-projecting GABAergic/CAMK2A neurons have been identified in the BNST and were
88 shown to produce rewarding and anxiolytic phenotypes upon optogenetic activation[11]. We
89 validated the presence of triple positive GABAergic/CAMK2A/CRH neurons in the aBNST
90 and CeA, by combining a recombinase-based intersectional mouse genetic strategy with CRH
91 immunohistochemistry (**Fig. 2b,c; Supplementary Fig.5**).
92 Next we labeled CAMK2A-expressing CRH neurons by injecting AAV-Camk2a::DIO-EYFP
93 into the aBNST and CeA of *Crh-ires-Cre* mice. Dendrites of CAMK2A/CRH neurons were
94 sparsely to moderately decorated with thin and mushroom-like spines, which received

95 presynaptic input evident by synaptophysin labeling (**Fig. 2d,e**). Moreover, we observed
96 dense EYFP labeling in fibers within the VTA and SNc following AAV-Camk2a::DIO-EYFP
97 injections into the CeA or aBNST (**Fig. 2f; Supplementary Fig. 6**). CLARITY of *Crh-ires-*
98 *Cre* mouse brains injected with AAV-Camk2a::DIO-EYFP additionally demonstrated that the
99 VTA/SNc represent primary projection targets of aBNST CAMK2A/CRH neurons (**Fig. 2g**;
100 **Supplementary Video 1**). Collectively, these results suggest that VTA-projecting CRH
101 neurons in the aBNST and CeA represent a previously undefined class of largely spiny,
102 CAMK2A-expressing, GABAergic long-range projection neurons. Although the majority of
103 CAMK2A/CRH neurons had spines, we were not able to accurately quantify the percentage
104 of total spiny vs. aspiny neurons due to the dense local projections and intermingled dendrites
105 of CeA/aBNST CRH neurons.

106 In order to target the identified CAMK2A/CRH circuit, we generated conditional *Crh*
107 knockout mice (Crh^{flox}), crossed them with $Camk2a\text{-}CreER^{T2}$ mice and induced the knockout
108 in adulthood via application of tamoxifen-containing food (**Fig. 3a**; **Supplementary Fig. 7**).
109 As expected, loss of *Crh* expression in $Crh^{CKO\text{-}Camk2a}$ mice was primarily observed in the
110 aBNST and CeA, but also in *Crh*-expressing glutamatergic neurons of the Pir (**Fig. 3b,c;**
111 **Supplementary Fig. 8a,b**). Based on our findings that deletion of *Crhr1* in dopaminergic
112 neurons increases anxiety[1], we assessed whether lack of *Crh* from VTA-projecting
113 CAMK2A/CRH neurons would result in similar effects. Compared to littermate controls,
114 $Crh^{CKO\text{-}Camk2a}$ mice displayed increased anxiety in the open field, dark-light box, elevated
115 plus-maze (EPM) and marble burying test, which was independent of altered corticosterone
116 release (**Fig. 3d-f; Supplementary Fig. 8c,d**). Importantly, the anxiogenic phenotype did not
117 result from *Crh* absence in *Camk2a*-expressing glutamatergic neurons, since deletion of *Crh*
118 specifically in glutamatergic neurons (Crh^{flox} × *Nex-Cre*) did not induce behavioral alterations
119 (**Supplementary Fig. 9**). In view of CRH's important role in conditioned fear[3] and recent
120 findings demonstrating that CeA CRH neurons mediate conditioned flight[12] and are required

for discriminative fear[9], we additionally assessed auditory and contextual fear conditioning. *Crh*$^{CKO\text{-}Camk2a}$ mice displayed increased freezing upon re-exposure to the tone (**Fig. 3g**), which was most prominent after termination of the conditioned stimulus. Notably, contextual fear memory was not altered (**Supplementary Fig. 8e**). Additional experiments revealed higher levels of sensitized fear to an unsignalled tone in *Crh*$^{CKO\text{-}Camk2a}$ mice, suggesting overall impairments in the readjustment of fear levels rather than alterations in fear memory formation (**Supplementary Fig. 8f-h**).

CRH is known to activate dopamine neuron firing and induce dopamine release[4,7,19], while deletion of *Crhr1* in dopaminergic neurons reduces dopamine release in the PFC[1], a structure critically involved in the modulation of anxiety and a major target of the mesocortical dopamine circuit. Applying in vivo microdialysis, we observed a significant reduction in absolute dopamine release in the PFC of *Crh*$^{CKO\text{-}Camk2a}$ mice, both under baseline conditions and following footshock stress (**Fig. 3h**). However, the magnitude of the response to the acute footshock was similar (**Supplementary Fig. 8j**), indicating generally lower dopamine levels in *Crh*$^{CKO\text{-}Camk2a}$ mice rather than alterations in stress-induced synaptic dopamine release. We detected no differences in dopamine levels in the nucleus accumbens (**Supplementary Fig. 8l**).

Next, we investigated potential compensatory changes in CRHR1/CRHR2 and Urocortin (UCN) expression in *Crh*$^{CKO\text{-}Camk2a}$ mice. qPCR analysis only revealed a significant upregulation of *Crhr1* in the VTA of *Crh*$^{CKO\text{-}Camk2a}$ mice, further supporting the involvement of CAMK2A-positive CRH neurons in CRHR1-VTA signaling (**Supplementary Fig. 8m**). To determine whether behavioral alterations in *Crh*$^{CKO\text{-}Camk2a}$ mice are caused by a lack of CRH from CAMK2A-positive aBNST/CeA neurons, or compensatory upregulation of *Crhr1* in the VTA, we explored the direct impact of enhanced CRH/CRHR1 signaling in the VTA on anxiety and fear conditioning. For this, we first generated a *Crhr1-ires-Cre* driver in which Cre-expression faithfully reproduces the endogenous *Crhr1* expression pattern without

147 compromising its expression and corticosterone release (**Supplementary Fig. 10 and 11**).
148 Using *Crhr1-ires-Cre* mice, we expressed a constitutively active version of CRHR1 fused to
149 EGFP (AAV-DIO-CA(CRHR1)-EGFP)[20] specifically in CRHR1-expressing VTA neurons
150 (**Fig. 3i; Supplementary Fig. 12a**). CA(CRHR1) mice exhibited decreased anxiety-related
151 behavior in the dark-light box, EPM and marble burying test (**Fig. 3j-l**), without displaying
152 changes in fear conditioning (**Fig. 3j-m, Supplementary Fig. 12**). This suggests that
153 enhanced CRHR1 signaling in the VTA promotes decreased anxiety without altering fear
154 memory expression. Similarly, intra-VTA microinjections of CRH (40 ng/side) in wild-type
155 mice partially decreased anxiety without altering fear levels. However, a lower dose of CRH
156 did not induce behavioral changes, while a higher dose significantly impaired locomotion
157 (**Supplementary Fig. 13**), indicating dose-specific effects on general behavior following
158 exposure to exogenous (potentially non-physiological) CRH levels. The fact that neither
159 VTA-specific expression of CA(CRHR1) nor microinjections of CRH affected cued freezing,
160 lets us speculate that increased fear memory expression in $Crh^{CKO\text{-}Camk2a}$ mice is a
161 consequence of CRH absence from locally projecting CeA neurons[9] and/or other long-range
162 projection neurons.
163 Notably, photo-excitation of VTA-innervating, ChR2-expressing CRH terminals did not alter
164 anxiety and fear memory expression (**Supplementary Fig. 14**). However, acute optogenetic-
165 mediated activation/inhibition of CRH fibers, which will likely impact the co-release of
166 GABA and presumably other neurotransmitters, cannot be directly compared to a chronic
167 manipulation of CRH alone. Consequently, our results imply that prolonged dysregulation of
168 CRH-release from VTA-targeting extended amygdala neurons, and/or chronic changes in
169 CRHR1 signaling in the VTA are required to induce alterations in anxiety-related behavior.
170 Importantly, previous work has repeatedly demonstrated an aversive/anxiogenic-like role for
171 CRH/CRHR1 signaling in the VTA of drug-experienced animals[5,8]. Thus, it is likely that

172 CRH release in the VTA can exert opposing effects on anxiety under baseline and drug/stress-

173 induced conditions[4].

174 Collectively our results suggest that a subpopulation of CRH/CAMK2A-expressing,

175 GABAergic projection neurons of the extended amygdala target CRHR1 on dopaminergic

176 VTA neurons to positively modulate emotional behavior by regulating dopaminergic

177 neurotransmission (**Supplementary Fig. 15**). This reveals a previously unidentified anxiolytic

178 CRH circuit and further establishes the presence of opposing CRH networks in the regulation

179 of stress-related emotional behavior.

180

181 **Acknowledgments**

182 We thank S. Bauer, C. Eggert, D. Harbich, M. Holzapfel, R. Hüttl, A. Mederer, A. Parl, A.
183 Ressle, R. Stoffel, L. Tietze, S. Unkmeir for excellent technical support, M. Eder for Core
184 Unit infrastructure and J. Keverne for manuscript proofreading. This work was partially
185 supported by the Max Planck Society, Volkswagen Foundation, German Federal Ministry of
186 Education and Research (FKZ:01ZX1314H to JMD, WW), Helmholtz Alliance ICEMED (to
187 WW), Chica and Heinz Schaller Foundation (to VG), DFG (SFB 1134 to VG), and FAPESP
188 (2013/03445-3 to KSG).

189

190 **Author contributions**

191 N.D. and C.K. designed and performed experiments and analyzed data. N.D. and J.M.D.
192 wrote the manuscript. M.J., J.H., K.S.G., M.L.P., S.C., A.K., A.M.V., M.W.M., B.S., and
193 R.C.A., assisted with behavioral and tracing/imaging experiments. E.A., J.D. and A.G.
194 conducted microdialysis, electrophysiology and optogenetic experiments respectively. K.J.R.,
195 C.T.W., V.G., A.C., M.V.S., W.W. and D.R. contributed to methodology and resources.
196 J.M.D. designed experiments, analyzed data and supervised the project.

197

198 **Competing interests**

199 The authors declare no competing financial interests.

200

201 **References**

202

203 1. Refojo, D. et al. *Science.* **333**, 1903–1907 (2011).

204 2. Swanson, L., Sawchenko, P., Rivier, J. & Vale, W. *Neuroendocrinology* **36**, 165–186
205 (1983).

206 3. Henckens, M.J.A.G., Deussing, J.M. & Chen, A. *Nat. Rev. Neurosci.* **17**, 636–651
207 (2016).

208 4. Lemos, J.C. et al. *Nature* **490**, 402–6 (2012).

209 5. Grieder, T.E. et al. *Nat. Neurosci.* **17**, 1751–1758 (2014).

210 6. Silberman, Y. & Winder, D.G. *Front. psychiatry* **4**, 42 (2013).

211 7. Wanat, M.J., Bonci, A. & Phillips, P.E.M. *Nat. Neurosci.* **16**, 383–5 (2013).

212 8. George, O., Le Moal, M. & Koob, G.F. *Physiol. Behav.* **106**, 58–64 (2012).

213 9. Sanford, C.A. et al. *Neuron* **93**, 164–178 (2016).

214 10. Haubensak, W. et al. *Nature* **468**, 270–6 (2010).

215 11. Jennings, J.H. et al. *Nature* **496**, 224–8 (2013).

216 12. Fadok, J.P. et al. *Nature* **542**, 96–100 (2017).

217 13. Rodaros, D., Caruana, D., Amir, S. & Stewart, J. *Neuroscience* **150**, 8–13 (2007).

218 14. Tagliaferro, P. & Morales, M. *J. Comp. Neurol.* **626**, 616–626 (2008).

219 15. Kubota, Y. *Curr. Opin. Neurobiol.* **26**, 7–14 (2013).

220 16. Yan, X., Toth, Z., Schultz, L., Ribak, C.E. & Baram, T.Z.**243**, 231–243 (1998).

221 17. Robison, A. J. *Trends Neurosci.* **37**, 653–662 (2014).

222 18. Robison, A.J. et al. *J. Neurosci.* **33**, 4295–307 (2013).

223 19. Wanat, M.J., Hopf, F.W., Stuber, G.D., Phillips, P.E.M. & Bonci, A. *J. Physiol.* **586**,
224 2157–70 (2008).

225 20. Garcia, I. et al. *Dev. Cell* **30**, 645–659 (2014).

226

227 **Figure legends**

228

229 **Figure 1** GABAergic CRH neurons in the aBNST and CeA project to the VTA and carry
230 dendritic spines. **(a, b)** Synaptophysin (Syp)-GFP in the aBNST and CeA (top), and
231 projections in the VTA (bottom) in *Crh-ires-Cre* mice; TH (dopaminergic marker tyrosine
232 hydroxylase). (**c**) *Crh* mRNA expression determined by ISH (left). Double ISH (brightfield,
233 right) - *Crh* (silver grains) is primarily expressed in GABAergic neurons (*Gad65/67*-positive,
234 red staining) of the adBNST and CeA. Black arrowheads, *Crh*-positive; grey arrowheads,
235 *Gad65/67/Crh*-positive. Quantifications in Supplementary Fig. 3. (**d**) Spiny and aspiny CRH
236 neurons in the aBNST and CeA of *Crh-ires-Cre;Ai32(ChR2-EYFP)* mice. Thin spines
237 (arrows), mushroom-like spines (arrowheads). Experiments in (a-c) and (d) were
238 independently replicated three and four times respectively. Abbreviations: anterior
239 commissure (ac), anterior dorsal BNST (adBNST), anterior ventral BNST (avBNST),
240 basolateral amygdala (BLA), central amygdala (CeA), ventral tegmental area (VTA).

241

242 **Figure 2** VTA-projecting spiny GABAergic CRH neurons express *Camk2a*. (**a**) *Crh* mRNA
243 expression determined by ISH (left panel). Double ISH – A subset of *Crh* neurons in the
244 adBNST and CeA co-express *Camk2a*. Black arrowheads, *Crh*-positive; grey arrowheads,
245 *Camk2a/Crh* double positive. Quantifications in Supplementary Fig. 3. (**b**) Schematic
246 representation of dual fate mapping strategy. Representative sections of *RC::FrePe*;*Dlx5/6-*
247 *Flp*;*Camk2a-CreER*^{T2} mice (**c**) and subsequent CRH immunostaining (red) show triple
248 positive GABAergic/CAMK2A/CRH neurons (arrowheads) in the CeA and aBNST. (**d**)
249 CAMK2A/CRH neurons carry thin (arrows) and mushroom-like (arrowheads) spines, which
250 receive presynaptic input determined by synaptophysin (SYP, red) immunostaining (**e**). (**f**)
251 CeA CAMK2A/CRH neurons (top) and VTA innervating fibers (bottom). (**g**) Whole brain
252 CLARITY; horizontal Z-stack image showing GABAergic, CAMK2A/CRH-positive aBNST-

253 VTA projections (arrowheads);video in Supplementary Information. All experiments were
254 independently replicated three times. Abbreviations: anterior BNST (aBNST), anterior dorsal
255 BNST (adBNST), anterior ventral BNST (avBNST), basolateral amygdala (BLA), central
256 amygdala (CeA) substantia nigra pars compacta (SNc), ventral tegmental area (VTA).

257

258 **Figure 3** CRH in CAMK2A neurons regulates anxiety, fear memory expression and
259 dopamine release in the prefrontal cortex. (**a**) Schematic illustration of the targeted *Crh* allele
260 (Crh^{flox}); details in Supplementary Fig. 7. (**b-c**) ISH - *Crh* mRNA deletion pattern in Crh^{CKO-}
261 ^{Camk2a} mice; quantifications from four independent experiments in Supplementary Fig. 8b. (**d**)
262 Dark-light box test - lit zone time ($t_{(23)} = 2.6$, *$p = 0.018$), lit entries ($t_{(23)} = 1.9$, $p = 0.068$);
263 unpaired two-tailed t-test, n = 12 Crh^{Ctrl}, 13 $Crh^{CKO\text{-}Camk2a}$. (**e**) Open arm time (%) in the EPM
264 ($t_{(18)} = 2.4$, $p = 0.031$; unpaired two-tailed t-test, n = 11 Crh^{Ctrl}, 9 $Crh^{CKO\text{-}Camk2a}$). (**f**) Marble
265 burying test ($t_{(31)} = 2.8$, **$p = 0.009$; Unpaired two-tailed t-test, n = 16 Crh^{Ctrl}, 17 Crh^{CKO-}
266 ^{Camk2a}). (**g**) Cued fear conditioning (RM ANOVA time × group interaction: $F_{(6,156)} = 3.88$, p =
267 0.0012; Bonferroni post hoc test, *$p < 0.05$, ***$p < 0.0001$; n = 13 Crh^{Ctrl}, 15 $Crh^{CKO\text{-}Camk2a}$.
268 (**h**) In vivo microdialysis showing decreased dopamine release in the prefrontal cortex of
269 $Crh^{CKO\text{-}Camk2a}$ mice under baseline conditions and following footshock (FS) stress (RM
270 ANOVA genotype effect: $F_{(1,17)} = 7.14$, *$p = 0.02$; n = 10 Crh^{Ctrl}, 9 $Crh^{CKO\text{-}Camk2a}$. (**i**) Cre-
271 dependent expression of a constitutively active (CA) CRHR1-EGFP fusion construct (AAV-
272 Ef1a::DIO-(CA)CRHR1-EGFP) in VTA neurons of *Crhr1-ires-Cre* mice (representative
273 images from three independent experiments; details in Supplementary Figures 11-12).
274 Littermate controls were injected with AAV-Ef1a::DIO-mCherry). *Crhr1-ires-Cre* mice
275 expressing (CA)CRHR1 in the VTA exhibit decreased anxiety in the (**j**) dark-light box test (lit
276 zone time: U = 14, *$p = 0.043$ / lit zone entries: U = 20, $p = 0.1$ / Mann Whitney U test two-
277 tailed; n = 7 Ctrl, 10 (CA)CRHR1), (**k**) EPM ($t_{(15)} = 2.2$, *$p = 0.043$; unpaired two-tailed t-
278 test; n = 7 Ctrl, 10 (CA)CRHR1) and (**l**) marble burying test ($t_{(17)} = 4.3$, ***$p = 0.005$;

279 unpaired two-tailed t-test; n = 8 Ctrl, 11 (CA)CRHR1) without showing alterations in (**m**)
280 cued fear conditioning (RM ANOVA time × group interaction: $F_{(6,102)} = 0.45$, $p = 0.84$; n = 8
281 *Ctrl*, 11 (CA)CRHR1). Abbreviations: Anterior dorsal BNST (adBNST), anterior ventral
282 BNST (avBNST), central amygdala (CeA), substantia nigra pars compacta (SNc), ventral
283 tegmental area (VTA), tyrosine hydroxylase (TH). Error bars represent s.e.m.
284

285 **Online Methods**

286

287 **Animals.** All animal experiments/protocols were legally approved by the ethical committee
288 for the Care and Use of Laboratory animals of the Government of Upper Bavaria, Germany..
289 All mice were group housed (max. 4 mice/cage) under standard laboratory conditions (22 ±
290 1°C, 55 ± 5% humidity) with a 12:12 h light:dark schedule with food and water provided *ad*
291 *libitum*. All experiments were performed in 10-14 week old male mice other than 1)
292 corticosterone measurements in *Crhr1-ires-Cre* mice, which were performed in female mice
293 (Supplementary Fig. 11d) and 2) VTA-expression of CA(CRHR1), which was performed in
294 6-9 week old male mice (Fig. 3i-j and Supplementary Fig. 12). Behavioral testing and
295 microdialysis were conducted between 8:30 am and 12:30 pm during the light cycle. Mice
296 were single housed one week prior to behavioral testing and hormone assessment. For all
297 experiments with inducible Cre recombinase lines, tamoxifen was given in food pellets (LAS
298 CRdiet CreActive TAM400, LASvendi) during postnatal weeks 10-12, and analyses were
299 performed 1-2 weeks later. Morphological assessment of CRH neurons was conducted in *Crh-*
300 *ires-Cre*[21] mice bred to *Ai9* (*R26*$^{CAG::loxP\text{-}STOP\text{-}loxP\text{-}tdTomato}$, stock no: 007905) or *Ai32*
301 (*R26*$^{CAG::loxP\text{-}STOP\text{-}loxP\text{-}ChR2\text{-}EYFP}$, stock no: 012569)[22] mice, which were purchased from the
302 Jackson Laboratory. Conditional *Crh* knockout mice (please refer to ´Generation of
303 conditional knockout mice´ below) lacking *Crh* ubiquitously, in glutamatergic and CAMK2A-
304 expressing neurons were generated by crossing *Crh*^{flox} mice with *Cre Deleter* (purchased from
305 TaconicArtemis, Cologne, Germany), *Nex-Cre*[23] and *Camk2a-CreER*^{T2} mice[24] respectively.
306 Intersectional fate-mapping was performed in RC::FrePe mice[25,26], bred to Dlx5/6-Flp[27]
307 (purchased from Jackson Laboratory, stock no: 010815) and *Camk2a-CreER*^{T2} mice.

308

309 **Generation of conditional *Crh* knockout mice.** Mice with a floxed *Crh* allele (*Crh*^{flox}) were
310 generated based on the previously described strategy used to generate *Crhr1*-reporter mice,

311 and conditional *Crhr1* knockout mice[28]. The targeting vector was constructed from a universal
312 shuttle vector with an inverted diphtheria toxin A (DTA) expression cassette for negative
313 selection. The shuttle vector comprises the following components, which were flanked by
314 *attP* sites, thereby enabling cassette exchange in embryonic stem (ES) cells subsequent to
315 homologous recombination (from 5' to 3'): 5′ homology arm including *Crh* exon 1, and the 5′
316 part of intron 1, upstream *loxP* site, first *frt* site, adenovirus splice acceptor (SA), *tau-LacZ*
317 (*tZ)* reporter gene equipped at its C-terminus with a *flag* tag, second *frt* site, and a reverse-
318 oriented *EM7*-neo positive selection cassette, including a bovine growth hormone
319 polyadenylation signal. Finally, downstream of the second *attP* site: a reverse-oriented PGK
320 promoter, a third *frt* site, the 3′ part of intron one as well as exon 2 with the downstream *loxP*
321 site inserted in the 3′ UTR, and the 3′ homology arm (see also **Supplementary Fig. 7**). The
322 linearized (*ScaI*) targeting vector was electroporated into TBV2 ES cells (129S2). Mutant ES
323 cells were identified by Southern blot analysis of genomic ES cell DNA digested with *EcoRI*
324 (5'-probe) and *BamHI* (3'-probe), respectively. Mutant ES cells were used to generate
325 chimeric mice by blastocyst injection. Male chimeras were bred to wild-type C57BL/6J mice
326 and germline transmission of the modified *Crh* reporter allele (Crh^{tz}) was confirmed by PCR
327 in F1 offspring. Breeding the Crh^{tz} reporter mice with transgenic *Flpe Deleter* mice[29] led to
328 deletion of the *tZ-neo* cassette and resulted in a conditional *Crh* allele (Crh^{flox}) leaving exon 2
329 flanked by *loxP* sites. Subsequent breeding to Cre driver lines resulted in conditional deletion
330 of the *loxP* flanked *exon 2* (Crh^{CKO}). Mice were of a mixed 129S2/Sv×C57BL/6J genetic
331 background.

332

333 **Generation of *Crhr1-ires-Cre* mice.** Mice expressing Cre recombinase under the control of
334 the *Crhr1* promoter were generated by using a recombinase-mediated cassette exchange
335 (RMCE) strategy. ES cell clones carrying a respective docking site in intron 2 of the *Crhr1*
336 gene were generated previously[28]. In contrast to the $Crhr1^{tZ}$ allele the ES clone used for

337 RMCE did not contain a *loxP* site 5′ of exon 2 (*Crhr1*$^{tZ-\Delta loxP}$; see also **Supplementary Fig.**
338 **10)** The *attB* site-flanked *Crhr1-Cre* recombinase expression unit encompassed from 5′to 3′:
339 *Crhr1* intron 2 (3′ of the original *Bgl*II insertion site) to exon 3 fused to the *Crhr1* cDNA
340 covering exons 4-13, an *ires-Cre* cassette with a bGH-pA, a *frt* site followed by a PGK pA
341 and hygromycin resistance cassette both in inverse orientation. PhiC31 integrase-mediated
342 cassette exchange resulted in insertion of the *Crhr1-Cre* expression unit into the right *attP* site
343 as verified by PCR and sequencing (*Crhr1*$^{tZ-iCre}$). Mutant ES cells were used to generate
344 chimeric mice which transmitted the modified *Crhr1* allele through the germline. The *tau-*
345 *LacZ* reporter and hygromycin selection cassette were removed by breeding to *FLPeR* mice[30].
346 Selective removal of both cassettes was demonstrated by PCR on genomic DNA from
347 offspring using primers A (Flipase-1-fwd) 5′-GAC-CTG-CAG-GAA-CCA-ACT-GT-3′, B
348 (Primer-2-Cre-rev) 5′-CAC-CCA-TGG-TTA-GTC-CCA-GT-3′, C (P-Cre-downs-fwd2) 5′-
349 AAT-AAT-AAC-CGG-GCA-GGG-GG-3′, D (Flipper-rev-1) 5′-CGA-CTA-GAG-CTT-
350 GCG-GAA-CCC-3′, E (P-PGK-fwd2) 5′-CCT-ACC-GGT-GGA-TGT-GGA-AT-3′, F (Cre-
351 fwd) 5′-GAT-CGC-TGC-CAG-GAT-ATA-CG-3′, G (Cre-rev) 5′-AAT-CGC-CAT-CTT-
352 CCA-GCA-G-3′, Thy1-F1 5′-TCT-GAG-TGG-CAA-AGG-ACC-TTA-GG-3′ and Thy1-R1
353 5′-CCA-CTG-GTG-AGG-TTG-AGG-3′ (see also **Supplementary Fig 10**). Mice were kept
354 on a mixed 129S2/Sv×C57BL/6J genetic background.
355
356 **Production of adeno-associated viruses (AAVs).** The synaptophysin-GFP coding sequence
357 (original construct[31]) was subcloned into a double floxed inverted open-reading frame (DIO)
358 vector under the control of the Ef1α promoter (Ef1a::DIO-eYFP, Addgene, #27056). The
359 Camk2a::DIO-EYFP construct was created by replacing the Ef1a promoter in the Ef1a::DIO-
360 EYFP construct with a 1.5 kb *Camk2a* promoter fragment. Packaging and purification of
361 recombinant (r) AAVs (Serotype 1/2) was conducted as previously described[32]. rAAVs titers
362 were ~10^{10} genomic copies per µl. The Ef1a::DIO-(CA)CRHR1-EGFP vector was kindly

363 provided by Benjamin Arenkiel[20,33] and packaged into $AAV_{1/2}$. $AAV_{1/2}$-Ef1a::DIO-mCherry
364 was used as a control (vector purchased from Addgene; www.addgene.org, plasmid #50462,
365 donated by Bryan Roth).
366
367 **Stereotactic surgeries:** For all experiments utilizing stereotactic surgeries (viral injections for
368 tracing experiments, optic fiber or guide cannula placements for CRH microinfusions and in
369 vivo microdialysis), mice were anesthetized with isoflurane (Floren®, Abbott), 2% v/v in O_2
370 and placed in a stereotaxic apparatus (TSE systems Inc., Bad Homburg, Germany) with
371 adapted components to allow mouse inhalation anesthesia. Post-surgery recovery included
372 Metacam supplementation, 0.25 mg/100 mL with drinking water, for 3 days after surgery,
373 with daily inspection of food intake. At the end of the experiments, mice were killed with an
374 overdose of isoflurane (Floren®, Abbott), transcardially perfused with PBS followed by 4 %
375 PFA, and brains removed for subsequent analysis. For viral injections, CRH-microinfusions
376 and optogenetic experiments, brains were sectioned (40 µm) using a vibratome (MICROM
377 HM 650V, Thermo Fischer Scientific) and accurate placements of microinjection cannulas
378 and optic fibers verified. For microdialysis experiments, brains were sectioned using a
379 cryostat (Leica CM 3000) and accurate probe placements verified.
380
381 **Viral injections and tracing analyses.** *Crh-ires-Cre* mice were unilaterally injected with
382 either AAV-Ef1a::DIO-Syp-GFP or AAV-Camk2a::DIO-EYFP into the dorsal and ventral
383 part of the anterior BNST (350 nl dorsal + 350 nl ventral), CeA (300 nl), PVN (250 nl), Pir
384 (250 nl) and PFC (400 nl) using a 33 gauge microinjection needle with a 10 microliter syringe
385 (Hamilton®) coupled to an automated microinjection pump (World Precision Instruments
386 Inc.) at 100 nl/min. Coordinates in mm from bregma were as follows: aBNST (A/P +0.15,
387 M/L ±0.8, D/V -4.25 and -4.75), CeA (A/P -1.0, M/L ±2.6, D/V -4.5), PVN (A/P -0.80, M/L

±0.25, D/V -4.75). At the end of the infusion, needles were kept on site for 10 min and then slowly withdrawn. Viral expression was assessed 4 weeks post-surgery.

Fluorogold (Fluorochrome, LLC) was dissolved as 1% W/V in 0.9% saline and 0.3 ul were injected unilaterally in the VTA. Retrobeads were obtained from Lumafluor Inc and injected (undiluted solution) at a volume of 100 nl. VTA coordinates in mm from bregma: A/P -3.0, M/L ± 0.6 and D/V 4.5. Mice were sacrificed and brains assessed 4 days after surgery.

Microdialysis and dopamine measurements. Microdialysis was performed as described previously[34]. Guide cannulas were implanted unilateral into the right mPFC (coordinates in mm from bregma: A/P +2.20, M/L +0.35 and D/V 1.50). One day before the experiment, CMA 11 metal free microdialysis probes with a cuprophane membrane of 2 mm length and o.d. of 0.2 mm (CMA Microdialysis) were inserted and connected to the perfusion lines consisting of FEP tubing and low-volume liquid swivel TCS2-23 (EiCOM). From the moment of insertion, probes were continuously perfused with sterile artificial cerebrospinal fluid (concentrations in mM: NaCl, 145; KCl, 2.7; $CaCl_2$, 1.2; $MgCl_2$, 1.0; Na_2HPO_4, 2.0; pH 7.4) at a flow rate of 0.3 µl/min.

On the experimental day, following a 1 h equilibration period, 20 min microdialysis fractions were constantly collected in cooled 300-µl microtubes (Milian AG) containing 2 µl of 0.1 M perchloric acid at a perfusion rate of 1.1 µl/min. The dead volume of the outlet line was compensated by a delay in fraction harvesting (10 min). Six consecutive baseline samples were collected. Thereafter, mice were placed into a custom-made shock chamber for a total of 5 min. After 180 s of habituation, animals underwent two electric FSs (1.5 mA, 2 s long) with a 60 s interval in-between. Animals remained in the shock chamber for another 60 s before being returned to their microdialysis home cages.

Dopamine content in the microdialysates was determined by reversed-phase high-performance liquid chromatography (HPLC) with electrochemical detection (UltiMate3000

414 HPLC system/Coulochem III, Thermo-Fischer Scientific). All reagents used for the
415 phosphate-citrate mobile phase (methanol 10 %, pH 5.6) were of analytical grade (Carl Roth
416 GmbH or MERCK KGaA). Monoamines were separated on an analytical column (C18,
417 150x3 mm, 3 um; YMC Triart, YMC Europe GmbH) at a flow rate of 0.4 mL/min. The
418 potentials of the working electrodes were set at 75 mV, +250 mV, and the guard cell potential
419 was set at +350 mV. Dopamine concentrations were calculated by external standard curve
420 calibration using the peak area for quantification. The detection limit for dopamine was 0.032
421 nM.
422
423 **Intra-VTA CRH infusions.** Stainless steel cannulas (8 mm) were inserted bilaterally above
424 the left and right VTA (A/P -3.2 mm, M/L ±0.5 mm, D/V -3.6 mm). A small screw was
425 drilled into the skull to fixate the protective helmet. The screw and the cannulas were fixed to
426 the skull by the application of dental cement (Paladur, Heraeus Kulzer). Following surgery,
427 animals were allowed to recover for one week. Mice were infused with 0.4, 40 or 400 ng
428 CRH (Bachem #H-2435.001, 1 mg) pro side dissolved in aCSF. 500 nl/side were delivered at
429 an infusion rate of 0.1 ul/min using injectors that protruded 1 mm beyond the cannulas.
430 Vehicle animals received aCSF only. Mice were tested 30 min post vehicle or CRH injection.
431 Separate cohorts (vehicle and CRH treated) were used for each CRH dose (0.4, 40 and 400
432 ng/side). Each behavioral test was performed on a separate day for each CRH dose tested. The
433 tests were conducted in the following order: OF, DaLi, EPM and fear conditioning.
434
435 **Optogenetic stimulation.** Optogenetic activation of CRH-positive terminals within the VTA
436 was performed in *Crh-ires-Cre* mice bred to ChR2-EYFP-expressing Ai32 mice. *Crh-ires-*
437 *Cre;Ai9(tdTomato)* mice were used as respective controls. Optic fibers (200 µm, NA 0.39,
438 Thorlabs CFML12L20 cut to 7 mm length) were implanted bilaterally above the VTA using
439 the following coordinates in mm: AP -3.2, ML ±0.55, - DV 3.8 with an angle of ±10° and

440 secured with dental acrylic (Paladur, Heraeus Kulzer). After the stereotaxic surgery, the
441 animals were left for 2 weeks to recover. The laser (Omikron LightHUB-4, 460 nm) output
442 power was adjusted to read 12 mW measured at the fiber tip. The laser was pulsed at 20 Hz
443 with 15 ms pulse width, using an external pulse stimulator (Master-8, A.M.P.I.). Bilateral
444 stimulation of freely-moving animals was achieved using a fiber-optic rotary joint
445 (FRJ_1x2i_FC-2FC, doric).

446 *DaLi test:* Laser stimulation was initiated 5-10 seconds before the animals were placed into
447 the dark compartment and lasted for 420 seconds.

448 *EPM:* The EPM was divided into three alternating 5-min epochs: laser stimulation off,
449 stimulation on, and stimulation off (OFF-ON-OFF epochs).

450 *Auditory/cued fear conditioning* was performed as described in the Fear Conditioning section
451 below. Optogenetic stimulation took place only during the second minute of tone presentation
452 (60 seconds). Freezing was scored with the tracking software ANY-maze (Stoelting Co.).

453

454 **VTA-specific expression of a constitutively active CRHR1.** *Crhr1-ires-Cre* mice were
455 bilaterally injected with AAV-Ef1a::DIO-(CA)CRHR1-EGFP or the control virus AAV-
456 Ef1a::DIO-mCherry in the VTA (0.3 ul/side) at a rate of 0.10 µl/min using a Neuros series
457 Hamilton syringe (Reno, NV) connected to micro injection pump (World Precision
458 Instruments). Coordinates in mm for VTA injections were: A/P -3.0, M/L ±0.6, D/V -4.6.
459 Behavioral experiments (OF, DaLi, EPM, Marble burying and fear conditioning as described
460 above) were started at least 3 weeks after surgery.

461

462 **Immunofluorescence staining.** Immunofluorescence staining was performed as previously
463 described[1]. Briefly, brain slices were permeabilized with PBS-TritonX-100 0.1%, blocked at
464 RT for 1 h in 5% BSA in PBS-TritonX-100 0.1%, and incubated o.n. (or longer) at 4°C with
465 the primary antibody. On the next day, slices were washed and incubated with the secondary

466 antibody for 2h at RT. After a final wash, brain slices were stained with DAPI and mounted
467 with anti-fading fluorescence VectaShield medium (Vector Laboratories). Primary antibodies:
468 anti-tyrosine hydroxylase (#P40101, 1:2000, PelFreez Biologicals), anti-synaptophysin
469 (#ab14692, 1:2000, Abcam), anti-CRH, 1:20000, 1 week incubation; obtained from Paul E.
470 Sawchenko, Salk Institute, CA). Specificity of the anti-CRH antibody has previously been
471 validated[35,36]. Secondary antibodies (1:2000): Alexa Fluor 594 goat anti-rabbit IgG (#A11037,
472 Invitrogen Life Technologies, Carlsbad, CA), Alexa Fluor 647 goat anti-rabbit IgG (#A21244,
473 Invitrogen Life Technologies, Carlsbad, CA).
474
475 **Image acquisition.** Images were captured with either a Zeiss Axioplan2 fluorescent
476 microscope and the Axio Vision 4.5 software, or an Olympus IX81 inverted laser scanning
477 confocal microscope and the Fluoview 1000 software. For confocal imaging, a Z-stack of
478 pictures of areas of interest was obtained with 0.4-1.2 µm step size and 800x800 to 1024 x
479 1024 pixel picture size. Images were analyzed with ImageJ (http://rsweb.nih.gov/ij/) and
480 Adobe Photoshop CS2.
481
482 **In situ hybridization (ISH) and double ISH.** Brains were sectioned coronally at 20 µm
483 using a cryostat (Microm, Walldorf, Germany). The sections were thaw-mounted onto
484 superfrost slides, dried, and kept at -80°C. Single and double ISH was performed as
485 previously described[1,37,38]. The following riboprobes were used: *Gad67*: 984-1940 bp of
486 NM_008077; *Gad65*: 753-1600 bp of NM_008078; *Vglut1* (Slc17a7): 1716-2332 bp of
487 NM_010484; *Vglut2* (Slc17a6): 2427-3006 bp of NM_080853.3; *Crh* (3'UTR): 2108-2370 bp
488 of AY128673; *Camk2a*: 2034-2903 bp of NM_177407.4; *Tomato*: 337-1026 bp of
489 NM_205769. Quantifications of double and single ISHs were performed blindly using the
490 freely available NIH ImageJ software (http://rsbweb.nih.gov/ij/).
491

492 **Clarity.** Mice were perfused with 20 ml of 0.1M PBS at 4°C, followed by 20 ml of a
493 hydrogel solution containing 4% acrylamide, 0.05% Bis, 0.25% VA-044 Initiator, 4% PFA
494 and 0.1M PBS at 4°C. Brains were extracted and incubated in hydrogel solution at 4°C for 3
495 more days, then incubated at 37°C for 3h until the hydrogel solution had polymerized.
496 Subsequently, the tissue was submitted to a clearing process, in which the sample was washed
497 in a clearing solution containing 200 mM boric acid and 4% sodium dodecyl sulfate with pH
498 8.5 for 2 days at 37°C. After one week of incubation in clearing solution at 37°C,
499 electrophoretic tissue clearing was performed for 5 days in the clearing solution at 37°C and
500 15V. Following another week of incubation in the clearing solution at 37°C, the sample was
501 washed 2 times for 24h with PBST (0.1% TritonX in 0.1M PBS). The cleared brain was
502 incubated in FocusClear (CelExplorer Labs Co., Hsinchu, Taiwan) for 2h before imaging with
503 a LaVision Light Sheet microscope (LaVision BioTec, Duisburg, Germany). A movie
504 compiled from individual Z-stack images was created with ImageJ (http://rsweb.nih.gov/ij/).
505
506 **Open field, Dark-light box, and elevated plus-maze (EPM) tests.** The open field test was
507 used to assess general locomotion and anxiety-related behavior, and was conducted in evenly
508 illuminated (<15 lux) square apparatuses (50 x 50 x 60 cm). The test duration was 15 min.
509 The dark-light box and EPM were employed to assess anxiety-related behavior. The dark-
510 light box test was performed for 5min in apparatus consisting of a secure black compartment
511 (<5 lux) and an aversive, brightly illuminated white compartment (700 lux). The EPM
512 consisted of a plus-shaped platform with four intersecting arms, elevated 37 cm above the
513 floor. Two opposing open (30 x 5 cm) and closed arms (30 x 5 x 15 cm) were connected by a
514 central zone (5 x 5 cm). Animals were placed in the center of the apparatus facing the closed
515 arm and were allowed to freely explore the maze for 5 min. Open arm time was calculated in
516 percent: open arm time (%) = open arm time (s) / (open arm time (s) + closed arm time (s)).

517 All experiments were analyzed using the automated video-tracking system ANYmaze
518 (Stoelting, Wood Dale, IL).
519
520 **Marble burying test.** Mice were placed into a housing cage (Green Line IVC Sealsafe PLUS
521 Mouse, Techniplast), filled with corn cob bedding (5 cm high), and containing 10 black
522 marbles, evenly distributed over the surface of the corn cob layer. After the cages had been
523 covered with flipped cage lids, animals were allowed to roam the cages freely for 1 hour. At
524 the end of the test period the number of buried marbles was assessed by an observer blind to
525 the genotype.
526
527 **Fear Conditioning**. Contextual and cued fear conditioning was performed in conditioning
528 chambers (ENV-307A, MED Associates Inc.,) as previously described[39]. Foot shock (FS)
529 delivery and context-dependent fear memory were assessed in a cubic-shaped chamber with
530 metal grid floors, which was thoroughly cleaned and sprayed with 70% Ethanol before the
531 animals were introduced (shock context). A neutral context consisting of a Plexiglas®
532 cylinder with bedding was used to investigate cued (tone-dependent) fear memory, which was
533 cleaned and sprayed with 1% acetic acid (novel context). For foot shock application (day 0)
534 mice were placed into the conditioning chamber for 3 min. After 180 sec, a sine wave tone
535 (80 dB, 9 kHz) was presented for 20 sec, which co-terminated with a 2 sec scrambled electric
536 foot shock of 1.5 mA. The mice remained in the shock chamber for another 60 sec. In order to
537 measure the freezing responses to the tone, mice were placed into the novel environment
538 (cylinder) on the following day (day 1). Three minutes later, a 3 min tone was presented (80
539 dB, 9 kHz). The animals were returned to their home cages 60 sec after the end of tone
540 presentation. Contextual fear was tested by re-exposing the animals to the shock context for 3
541 min on day 2. As a measure of fear memory, freezing behavior was recorded and analyzed by
542 an observer blind to genotype. Freezing was scored if the animals adopted an immobile

543 posture (except for breathing-related movement) with all 4 paws on the ground and the head
544 in a horizontal position. Data were analyzed in 20-s, 60-s or 180-s bins and normalized to the
545 observation interval as indicated in the Results section.
546
547 **Pain perception and shock-related fear sensitization.** Individual pain thresholds were
548 essentially as described before[40,41]. In brief, on day 0 mice from a new cohort were
549 individually placed into the shock chamber. After 3 min baseline, current intensity of the foot
550 shock was constantly increased at 5 µA/s until the mice showed first signs of discomfort
551 (backwards moving; PT1) and pain (jumping and vocalization; PT2) and the respective
552 current intensities were noted. Once mice showed those signs of pain, the current was
553 immediately switched of. Behavioral performance was judged by trained observers blinded to
554 genotype.
555 To further investigate shock-related fear sensitization, all mice received an unsignalled
556 electric foot shock of 1.5 mA (2s) within 15s after determination of PT2 on day 0, and
557 returned to their home cages 60 s later. The next day (day 1), animals were placed into the
558 novel context. After a baseline period of 3 min, a sine-wave tone (9 kHz, 80 dB, 3 min) was
559 presented for the first time, and mice were placed back to their home cage 60 s after tone off-
560 set. This procedure allows to measure non-associative memory components of the
561 conditioning procedure[39,42–45]. On day 2, mice were re-exposed to the shock chamber for 3
562 min. Generalization of contextual fear was assessed by comparing the freezing responses
563 shown (i) before shock presentation at day 0, (ii) during exposure to the novel context before
564 the subsequent tone presentation (day 1) and (iii) during re-exposure to the shock context (day
565 2). Freezing behavior was recorded and analyzed by an observer blind to the genotype as
566 described above.
567

568 **Corticosterone measurements.** Plasma corticosterone concentrations were measured as
569 previously described[1] using the commercially available RIA kit (MP Biomedicals, Eschwege,
570 Germany) according to the manufacture's manual.
571
572 **qPCR analysis.** Tissue punches for respective brain regions were collected from coronal
573 cryosections with a punching tool (FST, 1 mm diameter), directly into ice-cold Trizol reagent
574 (Invitrogen), and stored at -80°C until RNA isolation. Total RNA was isolated following the
575 Trizol protocol and the aqueous phase was purified using Qiagen RNAeasy columns and
576 buffers. RNA templates were transcribed into cDNA with the Superscript III kit (Invitrogen)
577 and random hexamer primers. cDNA was amplified on a Roche LightCycler 96 System with
578 Fast SYBR Green PCR Master Mix (Roche). Specific primers and *Hprt* house-keeping
579 primers were as follows: *Crhr1* (fwd. 5´-GGG-CCA-TTG-GGA-AAC-TTT-A-3´; rev. 5´-
580 ATC-AGC-AGG-ACC-AGG-ATC-A-3´), *Ucn1* (fwd. 5´-TCT-TGC-TGT-TAG-CGG-AGC-
581 G-3´; rev. 5´-TCG-AAT-ATG-ATG-CGG-TTC-TGC-3´), *Hprt* (fwd. 5´-GTT-CTT-TGC-
582 TGA-CCT-GCT-GGA-3´; rev. 5´-TCC-CCC-GTT-GAC-TGA-TCA-TT-3´).
583
584 **Electrophysiological recordings.**
585 Brain slices were prepared as described before[46] in carbogenated choline chloride-based
586 solution. 300 μm slices at the level of the CeA were hemisected along the midline and
587 afterwards, incubated for 30 min in carbogenated artificial cerebrospinal fluid (aCSF) at 34°C.
588 After 60 min recovery at room temperature, a hemislice was transferred and submerged in the
589 recording chamber in which it was continuously perfused (4-5 mL/min) with aCSF at room
590 temperature. Patch-clamp recordings were carried out at 25°C as previously described[46]. The
591 patch-clamp electrodes (open-tip resistance 5-7 MΩ) were filled with a solution consisting of
592 (in mM): 130 K-Gluconate, 5 NaCl, 2 $MgCl_2$, 10 HEPES, 0.5 EGTA, 2 Mg-ATP, 0.3 Na-
593 GTP, 5 D-Glucose, 20 Na2-Phosphocreatine (pH 7.2 with KOH, liquid junction potential of

594 12 mV). ChR2 was activated by a Sapphire 488 nm laser (75 mW max. output power,
595 Coherent)[46]. Offline analysis was performed using the Pulse and Igor Pro softwares.
596
597 **Statistical analyses**. All results are presented as mean ± standard error of the mean (s.e.m.)
598 and were analyzed by the commercially available GraphPad Prism 7 software (GraphPad
599 Inc.). Statistical significance was defined as $p < 0.05$. Normality and equality of variance were
600 analyzed with the D'Agostino-Pearson omnibus test and Bartlett's test respectively. In cases
601 were sample sizes were too small, data distribution was assumed to be normal. Based on the
602 results of these tests, appropriate parametric (two-tailed unpaired t test) or non-parametric
603 (Mann-Whitney U test) tests were performed. Time-dependent measures assessed during
604 microdialysis, fear conditioning and optogenetic experiments were analyzed with repeated
605 measures ANOVA followed by Bonferroni post hoc analysis. No statistical methods were
606 used to predetermine sample sizes. Sample sizes were based on those reported in previous
607 publications[1,4,37,38,47–50]. Animals were randomly allocated into different experimental groups.
608 Conditional knockout mice and control littermates were assigned to the experimental group
609 on the basis of genotype. No specific randomization method was used. Age-matched
610 littermates were used as controls in all experiments. For behavioral analysis, experimenters
611 were blind to experimental conditions. Injection sites and viral expression were confirmed for
612 all animals by experimenters blinded to behavioral results. Mice showing incorrect cannula
613 placement, injection sites or optic fiber placement were excluded from analysis by
614 experimenters blinded to treatment.
615
616 **Life Sciences Reporting Summary.**
617 Further information on experimental design is available in the Life Sciences Reporting
618 Summary.
619

620 **Data and code availability.**

621 The data that support the findings of this study are available from the corresponding author 622 upon reasonable request. No custom or open source code was used for data collection and 623 analyses.

624

625 **References Methods**

626

627 21. Taniguchi, H. et al. *Neuron* **71**, 995-1013 (2011).

628 22. Madisen, L. et al. *Nat. Neurosci.* **15**, 793–802 (2012).

629 23. Goebbels, S., Bormuth, I., Bode, U., Hermanson, O. & Schwab, M.H. *Genesis* **44**, 611–

630 621 (2006).

631 24. Erdmann, G., Schütz, G. & Berger, S. *BMC Neurosci.* **8**, 63 (2007).

632 25. Brust R.D. et al. *Cell Reports*. 9, 2152-2165 (2012).

633 26. Bang, S., Jensen, P., Dymecki, S. & Commons, K. *Eur. J. Neurosci.* **35**, 85–96 (2012).

634 27. Miyoshi, G. et al. *J. Neurosci.* **30**, 1582–1594 (2010).

635 28. Kühne, C. et al. *J. Comp. Neurol.* **520**, 3150–80 (2012).

636 29. Rodríguez, C. et al. *Nat. Genet.* **25**, 139–140 (2000).

637 30. Farley, F., Soriano, P., Steffen, L. & Dymecki, S. *Genesis* **28**, 106–110 (2000).

638 31. Grinevich, V., Brecht, M. & Osten, P. *J. Neurosci.* **25**, 8250–8 (2005).

639 32. Pilpel, N., Landeck, N., Klugmann, M., Seeburg, P. & Schwarz, M. *J. Neurosci.*

640 *Methods* **182**, 55–63 (2009).

641 33. Nielsen, S.M., Nielsen, L.Z., Hjorth, S.A., Perrin, M.H. & Vale, W.W.

642 *Proc.Natl.Acad.Sci.U.S.A* **97**, 10277–10281 (2000).

643 34. Anderzhanova, E. a et al. *Eur. J. Pharmacol.* **708**, 95–104 (2013).

644 35. Chen, Y., Molet, J., Gunn, B.G., Ressler, K. & Baram, T.Z. *Endocrinology* **156**, 2015–

645 1673 (2015).

646 36. Muglia, Jacobson, Dikkes, M. *Nature* **373**, 427–432 (1995).

647 37. Dedic, N. et al. *Mol. Psychiatry* **23**, 533-543 (2018).

648 38. Hartmann, J. et al. *Mol Psychiatry* **22**, 466–475 (2016).

649 39. Kamprath, K. & Wotjak, C.T. *Learn. Mem.* **11**, 770–786 (2004).

650 40. Siegmund, A., Langnaese, K. & Wotjak, C.T. *Behav. Brain Res.* **157**, 291–298 (2005).

651 41. Thoeringer, C.K. et al. *Genes, Brain Behav.* **9**, 947–957 (2010).

652 42. Kamprath, K. et al. *J. Neurosci.* **26**, 6677–6686 (2006).

653 43. Kamprath, K. et al. *Genes, Brain Behav.* **8**, 203–211 (2009).

654 44. Siegmund, A. & Wotjak, C.T. *J. Psychiatr. Res.* **41**, 848–860 (2007).

655 45. Siegmund, A. et al. *J. Psychiatr. Res.* **43**, 1156–65 (2009).

656 46. Dine, J. et al. *Front. Cell. Neurosci.* **10**, 1–11 (2016).

657 47. Vogl, A.M. et al. *Nat. Neurosci.* **18**, 239–251 (2015).

658 48. Wang, X. D. et al. *Nat. Neurosci.* **16**, 706–13 (2013).

659 49. Walsh, J.J. et al. *Nat. Neurosci.* **17**, 27–9 (2014).

660 50. Pomrenze, M.B. et al. *Front. Neurosci.* **9**, 1–14 (2015).

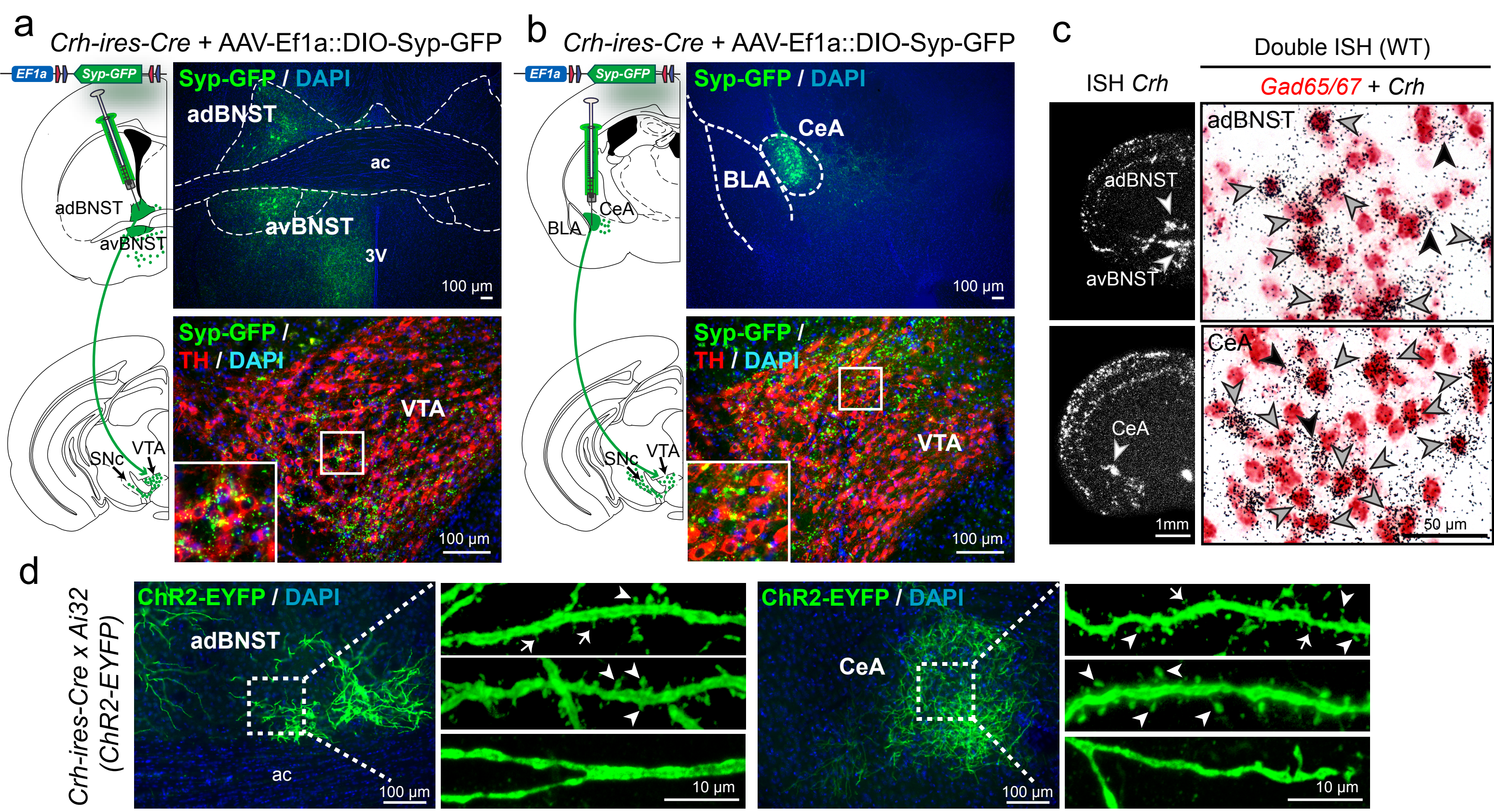
a
Crh-ires-Cre + AAV-Ef1a::DIO-Syp-GFP
EF1a
Syp-GFP
Syp-GFP / DAPI
adBNST
ac
avBNST
3V
100 µm
Syp-GFP / TH / DAPI
VTA
SNc
VTA
100 µm
b
Crh-ires-Cre + AAV-Ef1a::DIO-Syp-GFP
Syp-GFP / DAPI
CeA
BLA
100 µm
Syp-GFP / TH / DAPI
VTA
SNc
VTA
100 µm
c
Double ISH (WT)
ISH Crh
Gad65/67 + Crh
adBNST
avBNST
1mm
CeA
50 µm
d
Crh-ires-Cre x Ai32 (ChR2-EYFP)
ChR2-EYFP / DAPI
adBNST
ac
100 µm
10 µm
ChR2-EYFP / DAPI
CeA
100 µm
10 µm

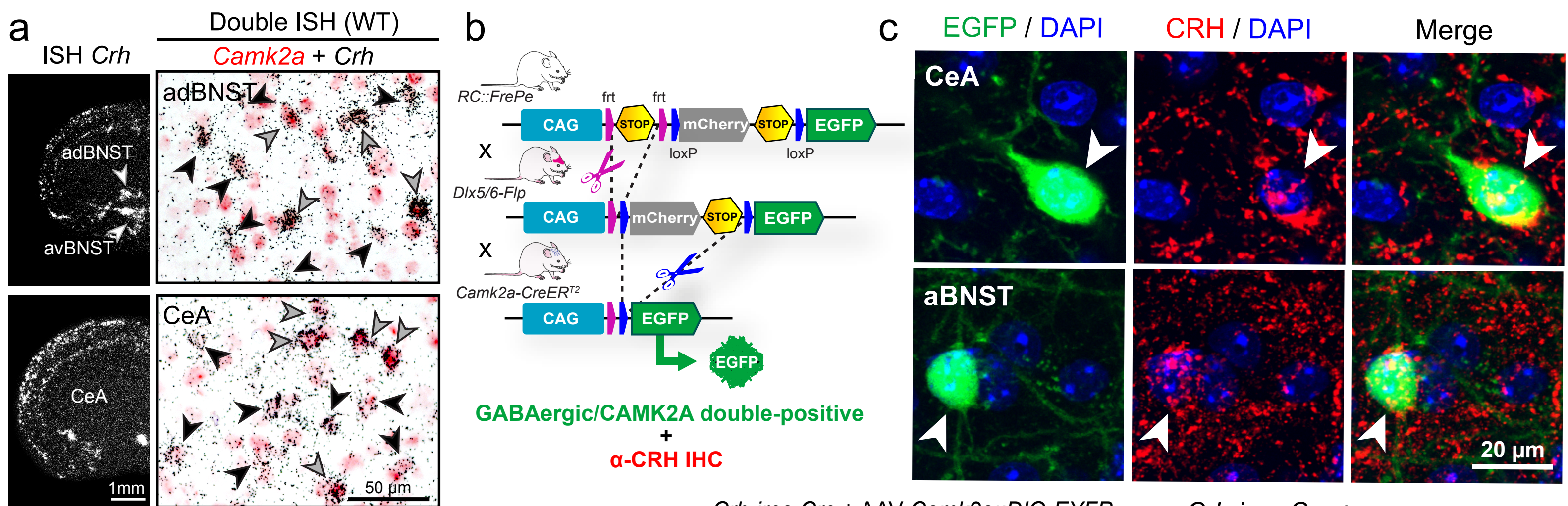
a
ISH Crh
Double ISH (WT)
Camk2a + Crh
adBNST
avBNST
CeA
1mm
50 µm
b
RC::FrePe
Dlx5/6-Flp
Camk2a-CreERT2
CAG
STOP
mCherry
EGFP
frt
loxP
GABAergic/CAMK2A double-positive
+
α-CRH IHC
c
EGFP / DAPI
CRH / DAPI
Merge
CeA
aBNST
20 µm

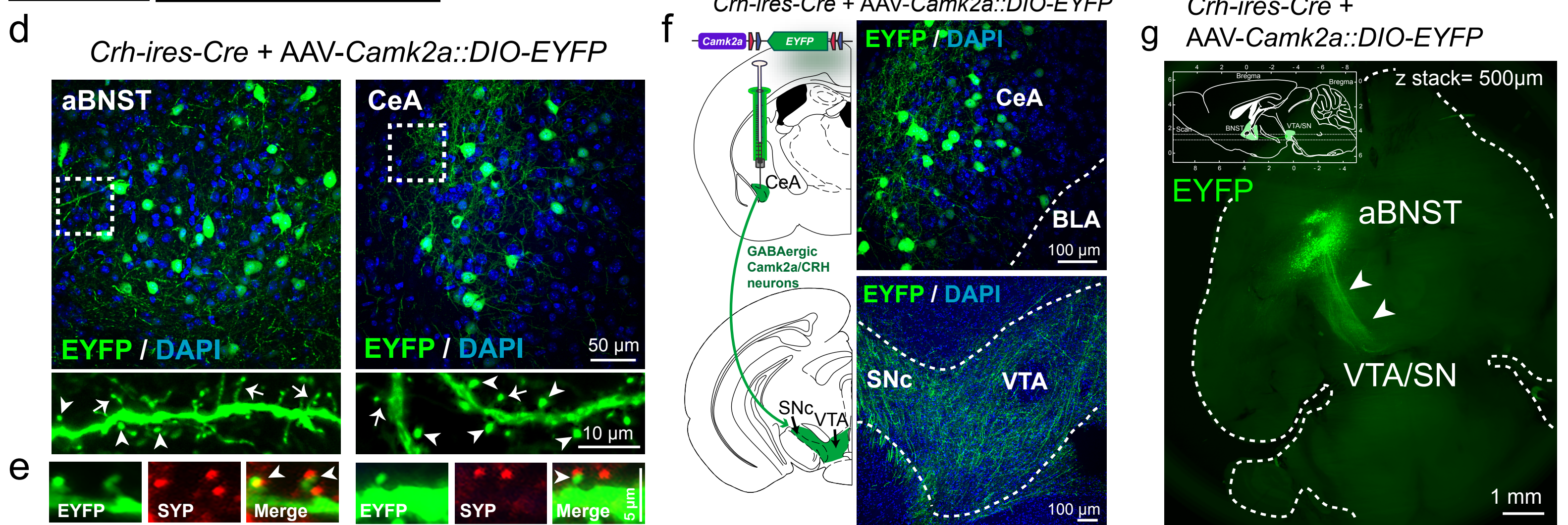
d
Crh-ires-Cre + AAV-Camk2a::DIO-EYFP
aBNST
CeA
EYFP / DAPI
50 µm
10 µm
e
EYFP
SYP
Merge
5 µm
f
Crh-ires-Cre + AAV-Camk2a::DIO-EYFP
Camk2a
EYFP
CeA
BLA
GABAergic Camk2a/CRH neurons
SNc
VTA
100 µm
g
Crh-ires-Cre + AAV-Camk2a::DIO-EYFP
z stack= 500µm
EYFP
aBNST
VTA/SN
1 mm

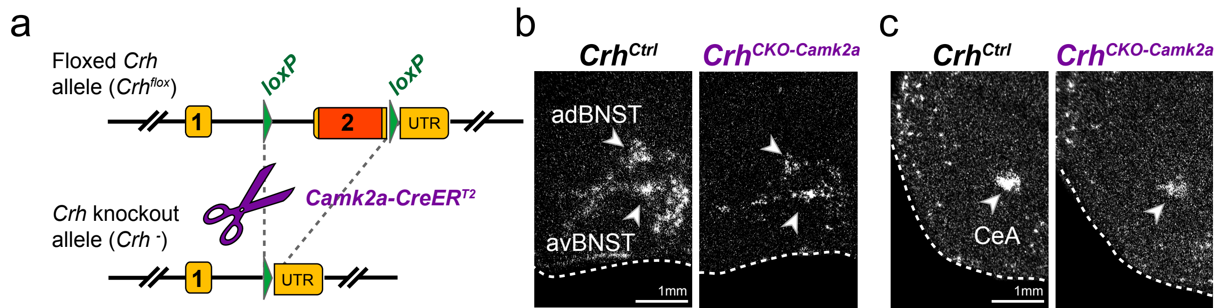
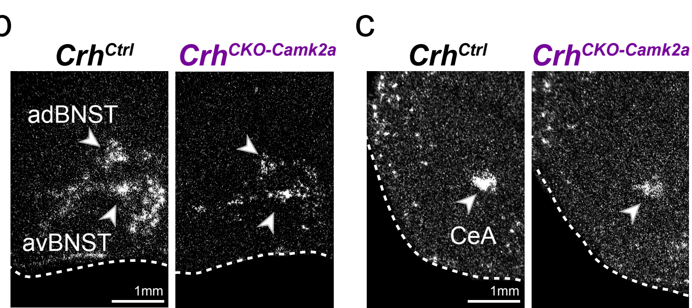
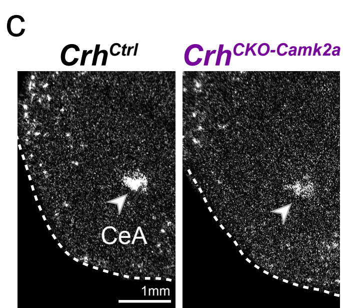
a
Floxed Crh allele (Crh^flox)
loxP
loxP
1
2
UTR
Camk2a-CreER^T2
Crh knockout allele (Crh -)
1
UTR
b
Crh^Ctrl
Crh^CKO-Camk2a
adBNST
avBNST
1mm
c
Crh^Ctrl
Crh^CKO-Camk2a
CeA
1mm

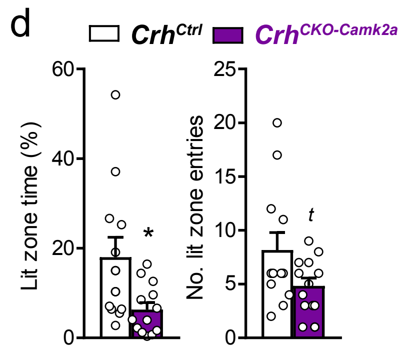
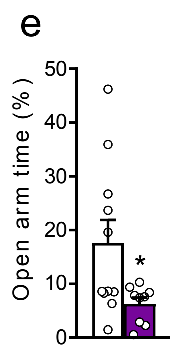
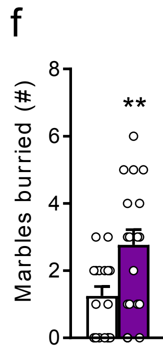
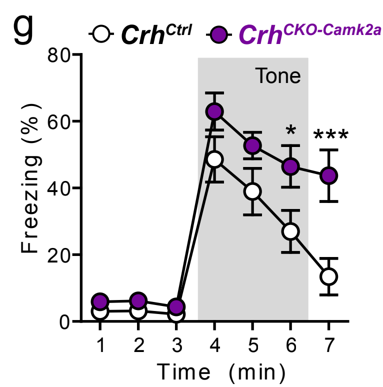
d
Crh^Ctrl
Crh^CKO-Camk2a
Lit zone time (%)
No. lit zone entries
e
Open arm time (%)
f
Marbles burried (#)
g
Freezing (%)
Tone
Time (min)

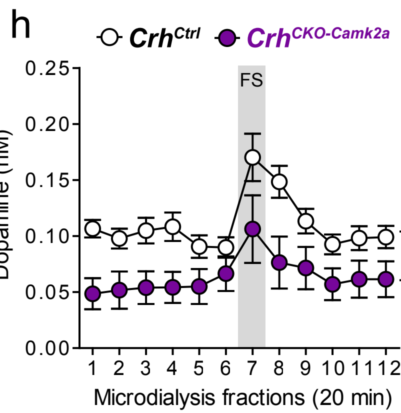
h
Crh^Ctrl
Crh^CKO-Camk2a
FS
Dopamine (nM)
Microdialysis fractions (20 min)

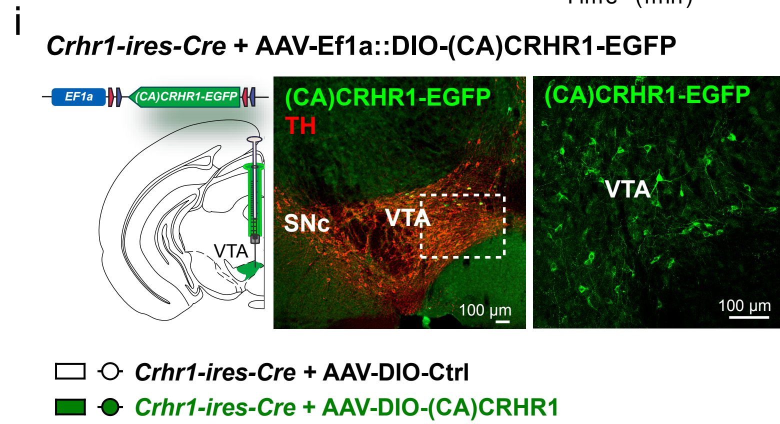
i
Crhr1-ires-Cre + AAV-Ef1a::DIO-(CA)CRHR1-EGFP
EF1a
(CA)CRHR1-EGFP
VTA
(CA)CRHR1-EGFP
TH
SNc
VTA
100 µm
(CA)CRHR1-EGFP
VTA
100 µm
Crhr1-ires-Cre + AAV-DIO-Ctrl
Crhr1-ires-Cre + AAV-DIO-(CA)CRHR1

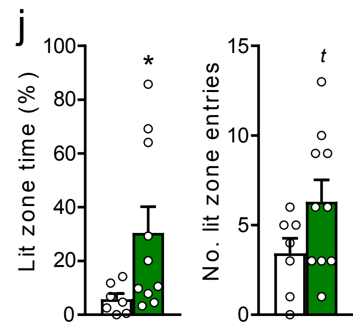
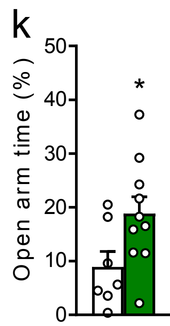
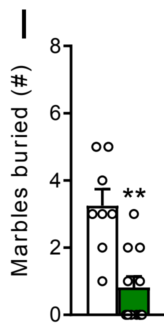
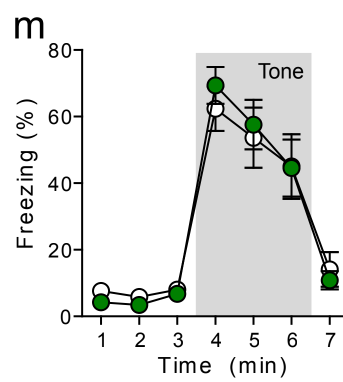
j
Lit zone time (%)
No. lit zone entries
k
Open arm time (%)
l
Marbles buried (#)
m
Freezing (%)
Tone
Time (min)